This article has been accepted for publication in IEEE Transactions on Power Systems. This is the author's version which has not been fully edited and content may change prior to final publication. Citation information: DOI 10.1109/TPWRS.2022.3187069

Rule-based Peak Shaving Using Master-Slave Level Optimization in a Diesel Generator Supplied Microgrid

Rampelli Manojkumar, *Student Member, IEEE*, Chandan Kumar, *Senior Member, IEEE*, Sanjib Ganguly, *Senior Member, IEEE*, Hoay Beng Gooi, *Life Senior Member, IEEE*, Saad Mekhilef, *Fellow, IEEE*, and João P. S. Catalão, *Fellow, IEEE*

***Abstract*—This paper proposes a rule-based peak shaving method using master-slave level optimization and presents its impact on an isolated diesel generator (DG) supplied microgrid. The DG is connected to low voltage (LV) ac bus through a back-to-back converter. This DG supplies power to a modified CIGRE residential distribution system which consists of residential loads and renewable energy sources (RESs). In such a system the fuel consumption of DG not only depends on the LV ac bus power requirement but also on its rated power. The rated power of DG can be reduced through the peak shaving application. In this scenario, a battery energy storage system (BESS) is connected at dc bus of the back-to-back converter for the peak shaving of DG power. The rule-based peak shaving method is proposed for determining BESS charge/discharge schedules considering the day-ahead LV ac bus powers over a day as inputs. For that firstly the LV ac bus powers are optimally obtained using a slave level optimization. In order to obtain the optimal peak DG power a master level optimization is used which determines the optimal control inputs for the rule-based control. The proposed peak shaving control method is tested in MATLAB.**

***Index Terms*—Battery energy storage systems, diesel generator, isolated microgrid.**

NOMENCLATURE

A. Notations

$\eta_c\{\eta_d\}$	Battery charging{discharging} efficiency
C_{dg}	Coefficient of DG energy to charge battery
e	Tolerance of regula falsi method
E^*_{b-d}	Dischargeable energy of battery
$E_{lvi-c}\{E_{dg-c}\}$	Available LV ac bus injected{DG} energy to charge battery over a day
$E_{b-c}\{E_{b-d}\}$	Required energy for charging{to be discharged by} battery over a day
E_{b-r}	Energy rating of battery
$E_r\{E_{phs}\}$	Energy generated by RESs{exported to PHS} over a day
FC_{dg}	Fuel consumption of DG
$n_l\{n_r\}$	Number of loads{RESs}
$P^l_{b-c}\{P^l_{b-d}\}$	Battery charge{discharge} power limit
$P_{lvi-c-b}\{P_{dg-c-b}\}$	LV ac bus injected{DG} power used to charge battery
$P_{lvi-c}\{P_{dg-c}\}$	Available LV ac bus injected{DG} power to charge battery
$P_{b-c}\{P_{b-d}\}$	Battery charge{discharge} power
$P_{dg-peak}$	Peak power drawn from DG over a day
P_{dg-r}	Power rating of DG
$P_{dgb-wcs}$	DG bus power in worst case scenario
$P_{dg}\{P_{phs}\}$	DG{pumped hydro storage} power
P_{loss}	Power loss
$P_{lvdl0}\{P_{dgbfil0}\}$	Operating LV ac bus demand{feed-in} limit
P_{lvdl1}, P_{lvdl2}	Initial LV ac bus demand limits
$P_{lvdl}\{P_{lvfil}\}$	LV ac bus demand{feed-in} limit
$P_{lvd}\{P_{lvi}\}$	LV ac bus demand{injection} power
P_{lv}, P_b, P_{dgb}	LV ac bus, battery and DG bus powers
$P_l\{P_{TL}\}$	Each load{total load} power
$P_{rc}\{Q_{rc}\}$	Active{reactive} power supplied by RES converter
P_{rs}	Power supplied by RES
pf_{rc-min}	Minimum Power factor of RES converters
$pf_{rc}\{S_{rc-r}\}$	Power factor{kVA rating} of RES converter
SCR	Self consumption rate of the system
$SoC_i\{SoC_f\}$	SoC at the start{end} of the day
$SoC_l\{SoC_u\}$	SoC lower{upper} limit
T	Forecast horizon
t	Time
t_1	Time slots when available optimal LV ac bus injected power to charge battery is more than LV ac bus feed-in limit
T_c	Each time slot duration

Manuscript received September 18, 2021; revised Jan 19, 2022, April 14, 2022 and May 25, 2022; accepted June 19, 2022. This work was supported in part by the ASEAN-India collaborative research project entitled "Design, control and management of distributed generation in microgrid" under Science & Engineering Research Board (SERB) and in part by the Central Power Research Institute (CPRI), India Research Project Entitled "Design, Operation, and Control of Distributed Generation (DG) Integrated Unified Power Quality Conditioner (UPQC) in Electric Grid". *(Corresponding author: Chandan Kumar).*

Rampelli Manojkumar, Chandan Kumar, and Sanjib Ganguly are with the Department of Electronics and Electrical Engineering, Indian Institute of Technology Guwahati, Guwahati 781039, India (e-mail: manoj023manoj@gmail.com; chandank@iitg.ac.in; sganguly@iitg.ac.in).

Hoay Beng Gooi is with the School of Electrical & Electronic Engineering, Nanyang Technological University (NTU), Singapore 639798, Singapore (e-mail:ehbgooi@ntu.edu.sg).

Saad Mekhilef is with the School of Science, Computing and Engineering Technologies, Swinburne University of Technology, Hawthorn, VIC 3122, Australia (e-mail:smekhilef@swin.edu.au; saad@um.edu.my).

João P. S. Catalão is with the Faculty of Engineering of the University of Porto and INESC TEC, Porto 4200-465, Portugal (e-mail:catalao@fe.up.pt).

t_d, t_c	Discharging mode and charging mode time slots
TFC_{dg}	Total fuel consumption of DG
V_{b-r}	Voltage rating of battery
$V_{lv}\{V_l\}$	LV ac{load} bus voltage
$V_{min}\{V_{max}\}$	Minimum{maximum} bus voltage limit

B. Indices

i	Index of loads
j	Index of RESs
o	Index of optimal value of the variables

I. Introduction

Isolated microgrids (MGs) are important to support the loads which are not connected to utility grid supply [1]. The isolated MGs depend on diesel generator (DG) for power supply due to their low installation cost, simple and reliable operation. However, the high operating cost is the main disadvantage of DGs which depends on its fuel consumption. The use of renewable energy sources (RESs) and battery energy storage systems (BESSs) is encouraged to avoid high operating cost of DGs [2]. In [3], the benefits of integrating BESS with DG such as system life improvement, fuel consumption reduction, and improved reliability of the power supply system are presented. In [4], [5], BESS is used along with RESs for minimizing the daily energy cost of the system which involves the fuel consumption of DG. In [6], optimal sizing of the RESs, BESS and DGs is done for minimizing the energy cost and life cycle cost of the system. In [7], optimal sizing of the RESs and BESS is done for minimizing the annual cost of DG based isolated system. The RESs like photovoltaiv (PV), wind power sources and BESS are connected through power converters to the distribution network. These power converters with their ability to operate in grid forming mode and grid following mode are known as smart power converters [8].

Several applications of smart power converters are presented in literature. The use of smart power converter to maintain constant ac bus voltage in DG based systems is presented in [9] and [10]. When a DG is used to supply power to an MG connected at low voltage (LV) ac bus, its fuel consumption mainly depends on the LV ac bus power. It is possible to reduce this LV ac bus power using smart power converters. In [11], the unified power quality conditioner is used to minimize power requirement of a distribution network. In [12], reactive power control strategies for minimizing the power requirement in a wind farm system are presented. In [13], the reactive power control through PV inverters is employed to minimize the power requirement while improving the voltage profile of distribution network. In [14], [15], smart power converters are operated in grid forming mode to reduce the load demand through LV ac bus voltage magnitude control. In [16], [17], the impact of voltage and reactive power control using smart power converters is presented for reducing the power requirement of the system.

However, considering the DG based systems it is not sufficient to reduce the power requirement of the system in order to reduce the fuel consumption. Because the fuel consumption depends on the rating of DG along with the power requirement [18]. The rating of DG can be reduced by the peak shaving control. In [19], an offline heuristic algorithm named MinPeak is developed to minimize the peak power consumption while scheduling the controllable appliances of the system. However, the application of the energy storage is not considered. In [20], an online computational approach is developed for minimizing the peak grid demand considering the electric vehicle (EV) charging. In [21], a heuristic algorithm is developed for minimizing the EV charging cost as well as the peak demand while controlling the charging powers of EV. However, the control of battery power during discharging is not discussed in [20], [21]. In [22], an online algorithm is proposed to minimize the peak demand usage while determining the discharge quantity of the energy storage. However, the control of battery power during charging is not considered.

Further, the peak shaving control using demand and feed-in limits with the application of the battery is presented in literature. The maximum limit of power that is drawn from (injected into) a bus is known as the demand limit (feed-in limit) at that bus. In [23], peak shaving is done through demand limit using coordinated control of PV and energy storage systems. In [24], energy storage is used for the peak shaving considering demand limit in order to enhance the reliability of supply. In [25], demand limit is considered to modify the load shape and minimize the energy cost of the system. In [26], demand limit is considered to operate the appliances of the system economically. In [27], the peak shaving is done while minimizing the operating costs of the system. The demand limit is considered as a constraint. The trajectory of state of charge (SoC) of the battery, set points of voltage regulating devices, and reactive powers DERs are considered as control variables. The optimization problem is formulated as mixed-integer second-order cone program which is handled by CPLEX solver. However, the number of control variables are more as the trajectories are considered to be controlled (e.g. considering the SoC trajectory as the control variable leads to twenty four control variables over a day with hourly dispatch of the battery). Moreover, in [19]–[27], the feed-in limit is not considered.

The importance of peak feed-in limit for voltage control in distribution systems is presented in [28]. In [29], the feed-in limit is considered for the peak shaving, but the demand limit is not considered. The efficiency of the system is improved with the consideration of both demand and feed-in limits. Recently, a rule-based peak shaving control with demand and feed-in limits is proposed in [30]. The method of determination of control inputs for the rule-based control is discussed. The control inputs are determined such that they depend on a single control variable known as the dischargeable energy of the battery. Further, the rules of the peak shaving control are formulated such that the battery schedules depend on the control inputs of the day. This avoids the consideration of the SoC trajectory as the control variable for minimizing the peak demand. Accordingly, the rule-based peak shaving control is optimized by determining the optimal control inputs while controlling the dischargeable energy of the battery. However, there are certain limitations in [30] as given follows.

1) The battery charge/discharge efficiencies and its power

limits are not considered while determining the control inputs and formulating the rules of the proposed control method.

2) The load and RESs power values are used as different inputs for deciding the charge/discharge modes of the battery. Accordingly the control inputs are determined and the rules for the peak shaving control are formulated. These are not applicable when there is only one input power such as net load power at a bus is available (e.g. DG supplying the LV ac bus power requirement).

Consideration of charge/discharge efficiencies, power limits of the battery and availability of one input power requires modifications to the rule-based peak shaving control proposed in [30]. Accordingly, in this paper the modified rule-based peak shaving control is proposed i.e., the charge/discharge modes of the battery, the control inputs and the rules of the peak shaving control are modified while addressing the limitations of [30].

Further, to the best of our knowledge the impact of the peak shaving control in a DG supplied MG is not discussed in the existing literature. To fill this research gap, in this paper the impact of the proposed peak shaving control on DG rating, fuel consumption of DG and self consumption rate of the system is presented. In summary the contributions of the paper are as follows:

1) To propose a rule-based peak shaving control using BESS while minimizing the LV ac bus power using the back-to back converter and RES converters.
2) To know the impact of the proposed rule-based peak shaving control on the DG rating, fuel consumption of DG over a day and self consumption rate of the system.

The remainder of the paper is organized as follows: Section II and III describe the system model and the overview of proposed control, respectively. Section IV discusses the slave level optimization. Section V presents the determination of operating modes and control inputs of rule-based peak shaving control. Section VI and VII discuss the determination of the battery schedules and master level optimization, respectively. The obtained results are presented in Section VIII and conclusions are given in Section IX.

II. System Model

The considered isolated DG supplied MG system is shown in Fig 1. The MG represents the modified CIGRE residential distribution system [10], [31]. The resistance and reactance of lines are chosen as per [31]. The different components of the system are discussed as follows:

A. Loads

There are different residential loads L1, L2, L3, L4 and L5 connected at bus 7, 8, 9, 10 and 11, respectively. The constant power loads are considered with an operating power factor of 0.85 lagging.

B. RESs

Wind power sources Wind 1, Wind 2 and Wind 3 are present at bus 8, 9 and 11, respectively. The PV source is connected at

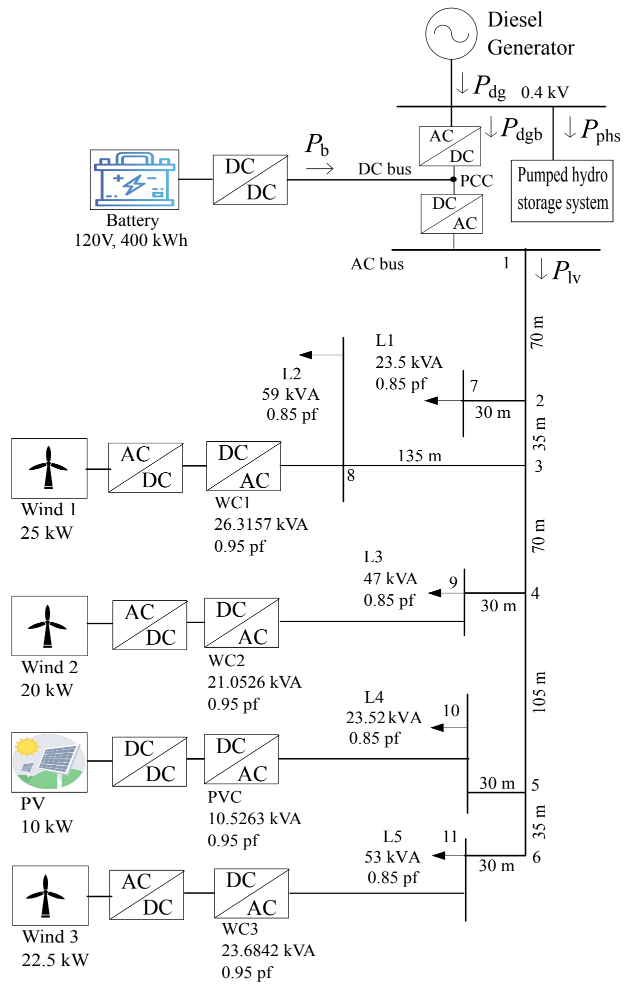

Fig. 1. Considered isolated MG system [10], [31].

bus 10. These RESs are connected through power converters to the load terminals. The dc/ac power converters used to connect RESs to the LV ac system i.e., WC1, WC2, PVC and WC3 are considered as RES converters.

C. RES Converters

RES converters are operated in grid-following mode to maintain the required active/reactive powers. The active power of the RES converters i.e., P_{rc}^j is considered the same as P_{rs}^j which is the maximum power point (MPP) power available from the RESs. The Q_{rc}^j is chosen optimally which will be discussed in following sections. The power balance equation at the LV ac bus with load and RES converters powers is given in (1).

$$P_{lv}(t) = \sum_{i=1}^{n_l} P_l^i(t) + P_{loss}(t) - \sum_{j=1}^{n_r} P_{rc}^j(t) \tag{1}$$

where t represents the time interval $[(t-1) \times T_c, t \times T_c]$ with T_c = 1 hour. The P_{lv} is used for obtaining P_{lvd} and P_{lvi} as given in (2) and (3), respectively

$$\begin{aligned} P_{lvd}(t) &= P_{lv}(t), \ \ P_{lv} > 0 \\ &= 0, \ \text{otherwise}. \end{aligned} \tag{2}$$

$$P_{lvi}(t) = -P_{lv}(t),\ P_{lv} \leq 0 \\ = 0,\ \text{otherwise.} \tag{3}$$

D. Back-to-back Converter

Back-to-back converter operating in grid forming mode is used to maintain the voltage and frequency at the LV ac bus as per the requirement. The frequency is maintained at 1 p.u. where as the LV ac bus voltage is optimally controlled which will be discussed in following sections.

E. Battery

Battery is connected at point of common coupling (PCC) i.e., dc bus of the back-to-back converter through a dc-dc converter. This converter is considered to be operating in grid following mode to maintain its power as per the required charge/discharge schedules. The P_b is given in (4),

$$P_b(t) = -P_{b-c}(t)/\eta_c,\ \forall t \in t_c \\ = P_{b-d}(t) \times \eta_d,\ \forall t \in t_d. \tag{4}$$

The charge/discharge schedules of the battery are obtained optimally using the proposed rule-based peak shaving control which will be discussed in following sections.

F. DG

The DG is used for balancing the deficit demand of the distribution system. It is connected to ac/dc converter of the back-to-back converter. The bus to which DG is connected is called as DG bus. The DG bus power i.e., $P_{dgb}(t)$ is determined using (5).

$$P_{dgb}(t) = P_{lv}(t) - P_b(t). \tag{5}$$

The P_{dg} is calculated using P_{dgb} as given in (6).

$$P_{dg}(t) = P_{dgb}(t),\ P_{dgb} > 0 \\ = 0,\ \text{otherwise.} \tag{6}$$

The fuel consumption of DG is given in (7).

$$FC_{dg}(t) = (a \times P_{dg}(t)) + (b \times P_{dg-r}) \tag{7}$$

where a and b are chosen as 0.246 L/kWh and 0.08415 L/kWh , respectively [32].

G. Pumped Hydro Storage (PHS)

If there is injected power available at DG bus, it can not be taken by DG. In general, the excess power available in the system is sent to either a dump load or any storage device if available in isolated MGs. Since the dump load is a combination of resistors, its usage leads to the wastage of excess power. To avoid this, in the considered system it is assumed that PHS is available to take care of the excess power [33]. In this work, the PHS is charged with the excess power available in the system after the optimal utilization of the battery. The PHS power depends on DG bus power (difference between distribution system power requirement and the battery power) as given in (8),

$$P_{phs}(t) = -P_{dgb}(t),\ P_{dgb} \leq 0 \\ = 0,\ \text{otherwise.} \tag{8}$$

The detailed operation and discharging phenomenon of PHS is not the scope of this paper.

III. Overview of the Proposed Peak Shaving Control

The overview of the proposed control is shown in Fig. 2. It includes various steps to realize the minimization of peak DG power which are discussed as follows.

Step 1: Day-ahead Forecasting of Load and RES Powers

The day-ahead forecasts of load and RES powers are required to determine the optimal LV ac bus powers. In recent years, several studies have been conducted for forecasting load and RESs power [34]. Data driven approaches for forecasting the RES and load power values have gained popularity due to the increased availability of monitoring data [35]. This monitoring data mainly includes weather forecast and historical energy usage data. Therefore, using the data driven approaches such as statistical and machine learning methods, the required day-ahead load and RESs power can be forecasted [36]. In this work, it is assumed that these forecasts are available. All the powers defined in the paper are obtained using these day-ahead forecasts which are further used to determine the day-ahead schedules of the battery.

Step 2: Slave Level Optimization

The slave level optimization is used to minimize the LV ac bus power while controlling the LV ac bus voltage and reactive power of RES converters at each time of the forecast horizon i.e., one day (T = 24 h). This is performed for the whole day in order to obtain the LV ac bus power curve over the day. The constraints of the optimization problem are load bus voltage magnitudes and RES converters ratings. Therefore, the slave level optimization helps in maintaining the load bus voltages within the grid code limits at all the times of the day. Moreover, the minimization of LV ac bus power through slave level optimization leads to the reduction of the power drawn from the DG which helps in the reduction of peak DG power.

Step 3: Determining the Operating Modes and Control Inputs for Rule-based Peak Shaving Control

The operating modes of the battery and control inputs for rule-based peak shaving are determined using the LV ac bus power curve of the day which is obtained through slave level optimization. The operating modes of the battery are chosen such that peak DG power is limited to the LV ac bus demand limit. The LV ac bus demand limit is defined as the optimal LV ac bus demand above which DG is not used to supply power to the system.

The control inputs for rule-based peak shaving are determined such that they depend on a control variable known as the dischargeable energy of the battery. The dischargeable energy of the battery is defined as the amount of energy that can be discharged from the battery over the forecast horizon without violating its power and SoC constraints. In this scenario, there exists a dischargeable energy of the battery which results in

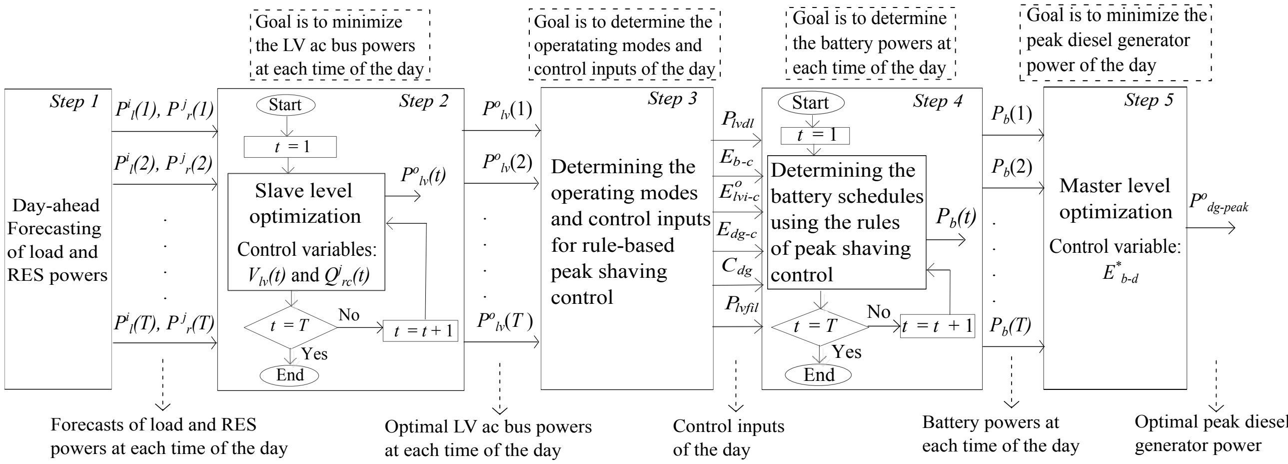

Fig. 2. Overview of the proposed peak shaving control.

minimum peak power over a day. It means that the control inputs of rule-based peak shaving control are same for the whole day corresponding to the dischargeable energy of the battery of that particular day. This indicates that the control inputs have to be determined only once per day.

Step 4: Determining the Battery Schedules Using the Rules of Peak Shaving Control

The rules of the peak shaving control are formulated based on the control inputs which are obtained in Step 3 to decide the charge/discharge schedules of the battery over a day.

Step 5: Master Level Optimization

The master level optimization minimizes the peak DG power while controlling the dischargeable energy of the battery. The control inputs corresponding to the optimal dischargeable energy of the battery are considered as the optimal control inputs for rule-based control.

From the aforementioned Steps 1-5, it can be seen that the master level optimization has to be done only once per day whereas the slave level optimization is performed twenty four times per day (for hourly dispatch of the battery). Also, it is not possible to solve master level optimization problem without the knowledge of the slave level optimization results of whole day. Because the peak power cannot be determined without knowing the powers of the whole day. Therefore, the master and slave level problems cannot be formulated as a single optimization problem as they are two separate problems which do not involve any decomposition.

These steps are explained in detail in following Sections.

IV. Slave Level Optimization

In this level, the LV ac bus voltage and RES converters are optimally controlled to minimize the power requirement of the LV ac bus for each time of the day. The fitness function is given in (9) and constraints are given from (10)-(13).

$$\text{minimize} \quad f = \sum_{i=1}^{n_l} P_l^i(t) + P_{loss}(t) - \sum_{j=1}^{n_r} P_{rc}^j(t). \quad (9)$$

subjected to

1) Power balance constraint

$$P_{lv}(t) = \sum_{i=1}^{n_l} P_l^i(t) + P_{loss}(t) - \sum_{j=1}^{n_r} P_{rc}^j(t). \quad (10)$$

2) Bus voltages constraint

$$V_{min} \leq V_l^i(t) \leq V_{max}. \quad (11)$$

3) RES converters constraints

$$pf_{rc-min} \leq pf_{rc}^j(t) \leq 1. \quad (12)$$

$$\sqrt{(P_{rc}^j(t))^2 + (Q_{rc}^j(t))^2} \leq S_{rc-r}^j. \quad (13)$$

The objective is to minimize the power drawn from the LV ac bus as given in (9). Equation (10) shows the power balance constraint at the LV ac bus neglecting power converters losses. Equation (11) indicates the load bus voltage magnitude constraint. The V_{min} and V_{max} are chosen as 0.95 p.u. and 1.05 p.u., respectively [37]. The constraints of power factor and kVA rating of RES converters are presented in (12) and (13), respectively. The pf_{rc-min} is chosen as 0.8. Note that the line thermal limits are not incorporated in optimization problem. They are assumed to be satisfied as the normal operation of the system is considered in this paper without any contingencies and the installed capacity of RES at each load is less than the rated load power. The chosen fitness function is a non-linear function. The genetic algorithm (GA) is a well-known meta heuristic optimization algorithm for solving complex nonlinear problems [38]. It has been successfully applied to solve real-life complex problems of various fields such as economics, engineering and management [39]. It maintains the diversity in population to avoid the solutions to stuck in local optima. Therefore, GA is used to solve this optimization problem. For GA it is important to choose parameters such as population size, rate of mutation and crossover etc., carefully to avoid any possible risk of non-convergence. The default values are chosen for various parameters of GA as per GA solver in MATLAB, except for population size [40].

The population size is an important parameter to choose. Because if it is small, the convergence might not be achieved and if it is big, the algorithm takes more time to get convergence. Therefore, population size is chosen based on the number of control variables. There are five control variables in this optimization i.e., the LV ac bus voltage and reactive power of RES converters. Further, in GA it is possible for different runs to provide different optimal values. Therefore, to avoid any sub-optimal solutions and guarantee global optimum solution the population size is tuned such that multiple simulation runs converge precisely to the same value and chosen as 50.

The control variables V_{lv} and Q^j_{rc} are chosen as given in (14) and (15)

$$0.95 \leq V_{lv}(t) \leq 1.05. \tag{14}$$

$$0 \leq Q^j_{rc} \leq (tan(cos^{-1}(pf_{rc-min})) \times S^j_{rc-r}). \tag{15}$$

The solution of the chosen optimization problem provides the optimal control variables and thereby optimal LV ac bus power values as output. These optimal LV ac bus power values obtained over a day are used as inputs to the proposed rule-based peak shaving control.

V. Determining the Operating Modes and Control Inputs for Rule-based Peak Shaving Control

A. Operating Modes

1) *Discharging Mode:* In order to limit $P_{dg}(t)$ to P_{lvdl}, the battery should be discharged whenever the optimal LV ac bus demand is more than the LV ac bus demand limit. Therefore, the discharging mode is during the time t_d when $P^o_{lvd}(t) > P_{lvdl}$.
2) *Charging Mode:* It is possible to charge the battery whenever the optimal LV ac bus demand is less than the LV ac bus demand limit. Therefore, charging mode is during the time t_c when $P^o_{lvd}(t) \leq P_{lvdl}$.

Now, the determination of control inputs of the rule-based peak shaving control is discussed as follows.

B. Control Inputs

The required inputs for the proposed rule-based peak shaving control are determined using the optimal LV ac bus power values obtained from the slave level optimization. The sequential order of determining these control inputs is shown in Fig. 3. The importance of each control input along with its determination process is discussed as follows.

1) LV ac Bus Demand Limit: In order to limit $P_{dg}(t)$ to P_{lvdl}, the battery has to supply the required power of $(P^o_{lvd}(t) - P_{lvdl})$ during discharging mode. However, considering discharging power limit, battery discharge power is given in (16),

$$\begin{aligned} P_{b-d}(t) &= (P^o_{lvd}(t) - P_{lvdl})/\eta_d, (P^o_{lvd}(t) - P_{lvdl}) \leq P^l_{b-d} \\ &= P^l_{b-d}, (P^o_{lvd}(t) - P_{lvdl}) > P^l_{b-d} \end{aligned} \tag{16}$$

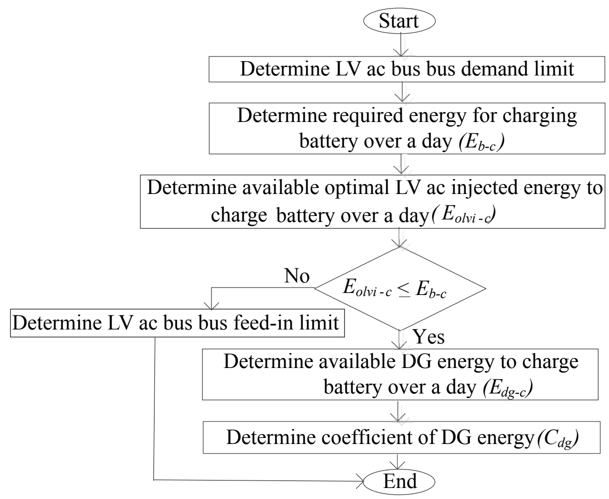

Fig. 3. Sequential order of determining control inputs of the proposed peak shaving control.

Then required energy to be discharged by the battery is determined as given in (17)

$$E_{b-d} = \sum_{t=1}^{T} P_{b-d}(t) \tag{17}$$

Now, the LV ac bus demand limit is determined such that the energy to be discharged by the battery is equal to the dischargeable energy of the battery i.e.,

$$E_{b-d} = E^*_{b-d}. \tag{18}$$

Here, the dischargeable energy of the battery is considered as a control variable which varies between 0 kWh and E_{b-r}.

$$0 \leq E^*_{b-d} \leq E_{b-r}. \tag{19}$$

From this range, E^*_{b-d} is chosen optimally through the master level optimization which will be discussed in following section. Substituting (17) in (18) gives

$$\sum_{t=1}^{T} P_{b-d}(t) - E^*_{b-d} = 0 \tag{20}$$

Equation (20) is in form of $f(P_{lvdl}) = 0$, with P_{lvdl} as independent variable. It means the problem of finding the LV ac bus demand limit becomes a root finding problem. In order to solve this, regula falsi method is used [30].

According to regula falsi method (P_{lvdl1}, P_{lvdl2}) are chosen such that $f(P_{lvdl1})$ is positive and $f(P_{lvdl2})$ is negative. Then, P_{lvdl0} is determined as follows.

$$\begin{aligned} P_{lvdl0} &= \frac{1}{m}(0 - f(P_{lvdl1})) + P_{lvdl1}, \text{ where} \\ m &= \frac{f(P_{lvdl2}) - f(P_{lvdl1})}{(P_{lvdl2} - P_{lvdl1})}. \end{aligned} \tag{21}$$

Using (21), we determine $f(P_{lvdl0})$. When $|f(P_{lvdl0})| < e$, P_{lvdl0} becomes P_{lvdl}. When $|f(P_{lvdl0}| > e$, either replace P_{lvdl1} by P_{lvdl0} if $f(P_{lvdl0}) > 0$ or replace P_{lvdl2} by P_{lvdl0} if $f(P_{lvdl0}) < 0$. Then, continue the above process till P_{lvdl0} becomes P_{lvdl}.

This article has been accepted for publication in IEEE Transactions on Power Systems. This is the author's version which has not been fully edited and content may change prior to final publication. Citation information: DOI 10.1109/TPWRS.2022.3187069

2) Required Energy for Charging the Battery Over a Day: For flexible day-to-day management, the battery has to be charged with same energy that is to be discharged by the battery. Therefore, required energy for charging the battery is equal to energy to be discharged by the battery over a day as given follows.

$$E_{b-c} = E_{b-d} = E^*_{b-d}. \tag{22}$$

3) Available Optimal LV ac Bus Injected Energy to Charge the Battery Over a Day: The required energy for charging the battery has to come either from the LV ac bus or DG. Firstly, available optimal LV ac bus injected energy to charge the battery is calculated. If it is not sufficient, then only available DG energy to charge the battery is determined and used for charging the battery. During t_c, the complete P^o_{lvi} is available for charging the battery as the optimal LV ac bus demand is less than the LV ac bus demand limit. However, considering the charging power limit, the available optimal LV ac bus injected power to charge the battery is given in (23),

$$\begin{aligned} P^o_{lvi-c}(t) &= P^o_{lvi}(t), P^o_{lvi}(t) \le P^l_{b-c} \\ &= P^l_{b-c}, P^o_{lvi}(t) > P^l_{b-c}. \end{aligned} \tag{23}$$

Then available optimal LV ac bus injected energy to charge the battery is determined as given in (24),

$$E^o_{lvi-c} = \sum_{t=1}^{T} P^o_{lvi-c}(t) \tag{24}$$

4) Available DG Energy to Charge the Battery Over a Day: When $E^o_{lvi-c} < E_{b-c}$, the deficit energy required for completely charging the battery is supplied by DG. Since DG power has to be limited to the LV ac bus demand limit, the available DG power to charge the battery is equal to P_{lvdl} subtracted by $P_{lvd}(t)$ which is given in (25),

$$\begin{aligned} P_{dg-c}(t) &= P_{lvdl} - P^o_{lvd}(t), \forall t \in t_c \\ &= 0, \text{ otherwise.} \end{aligned} \tag{25}$$

Then available DG energy to charge the battery is determined using (26),

$$E_{dg-c} = \sum_{t=1}^{T} P_{dg-c}(t). \tag{26}$$

5) Coefficient of DG Energy to Charge the Battery: When $E^o_{lvi-c} < E_{b-c}$, the DG has to supply only the deficit energy of $E^o_{lvi-c} - E_{b-c}$ over a day to the battery for flexible day-to-day management. It means the total available DG energy for charging the battery is not required to be supplied to the battery. In this case a coefficient known as coefficient of DG energy to charge the battery (C_{dg}) is considered which is determined as follows.

$$\begin{aligned} C_{dg}E_{dg-c} &= E_{b-c} - E^o_{lvi-c} \\ C_{dg} &= \frac{E_{b-c} - E^o_{lvi-c}}{E_{dg-c}}. \end{aligned} \tag{27}$$

6) LV ac Bus Feed-in Limit: When $E^o_{lvi-c} \ge E_{b-c}$, the complete available optimal LV ac bus injected energy is not required to be used for charging the battery. In this case, an LV ac bus feed-in limit is considered. This LV ac bus feed-in limit is the available optimal LV ac bus injected power to charge the battery below which the battery charging is not done. It means the available optimal LV ac bus injected power is not used to charge the battery whenever $P^o_{lvi-c}(t) \le P_{lvfil}$. Therefore, the battery is charged with $P^o_{lvi-c}(t) - P_{lvfil}$ whenever $P^o_{lvi-c}(t) > P_{lvfil}$ during t_c i.e.,

$$\sum (P^o_{lvi-c}(t) - P_{lvfil}) = E_{b-c}, \forall t \in t_c \&\& t_1, \tag{28}$$

where symbol '&&' indicates logical AND operator. Then,

$$\sum (P^o_{lvi-c}(t) - P_{lvfil}) - E_{b-c} = 0, \forall t \in t_c \&\& t_1. \tag{29}$$

Equation (29) is in form of $f(P_{lvfil}) = 0$, where

$$f(P_{lvfil}) = \sum (P^o_{lvi-c}(t) - P_{lvfil}) - E_{b-c}, \forall t \in t_c \&\& t_1. \tag{30}$$

In (29), P_{lvfil} is an independent variable. It is solved using the root finding algorithm of the regula falsi method which is similar to the determination of LV ac bus demand limit.

VI. Determining the Battery Schedules Using the Rules of Peak Shaving Control

The rules to determine the charge/discharge schedules of the battery are formulated to limit DG power and PHS powers to the corresponding LV ac bus demand and feed-in limits, respectively. These rules are presented as follows.

Rule 1: During t_d, the battery discharges by the amount $P_{b-d}(t)$ as per (16) to limit P_{dg} to P_{lvdl}.

Rule 2: During t_c, if $E^o_{lvi-c} \le E_{b-c}$ both the optimal LV ac bus injected power and DG power are used to charge the battery i.e., $P_{b-c}(t) = P^o_{lvi-c-b}(t) + P_{dg-c-b}(t)$. Here $P^o_{lvi-c-b}(t) = P^o_{lvi-c}(t)$ and $P_{dg-c-b}(t) = C_{dg}P_{dg-c}(t)$ as per (23) and (27).

Rule 3: During t_c, if $E^o_{lvi-c} > E_{b-c} \&\& P^o_{lvi-c}(t) > P_{lvfil}$, only the optimal LV ac bus injected power is used to charge the battery i.e., $P_{b-c}(t) = P^o_{lvi-c-b}(t)$. Here $P^o_{lvi-c-b}(t) = P^o_{lvi-c}(t) - P_{lvfil}$ as per (23) and definition of the LV ac bus feed-in limit.

Rule 4: During t_c, if $E^o_{lvi-c} > E_{b-c} \&\& P^o_{lvi-c}(t) \le P_{lvfil}$, the battery is not charged by either the optimal LV ac bus injected power or DG power i.e., $P_{b-c}(t) = 0$ as per the definition of the LV ac bus feed-in limit.

This process of determination of charge/discharge schedules of the battery using the above rules is shown as flowchart in Fig. 4. The SoC of the battery during discharging and charging modes is calculated using coulomb-counting method.

Now, the master level optimization which is used for determining the optimal control inputs for the rule-based peak shaving control is discussed as follows.

VII. Master Level Optimization

In this level, the optimal control inputs are determined to minimize the peak power of DG. The fitness function is given in (31) and constraints are given from (32)-(36),

$$\text{minimize} \quad f = P_{dg-peak} = \text{ maximum}(P_{dg}(t)). \tag{31}$$

This article has been accepted for publication in IEEE Transactions on Power Systems. This is the author's version which has not been fully edited and content may change prior to final publication. Citation information: DOI 10.1109/TPWRS.2022.3187069

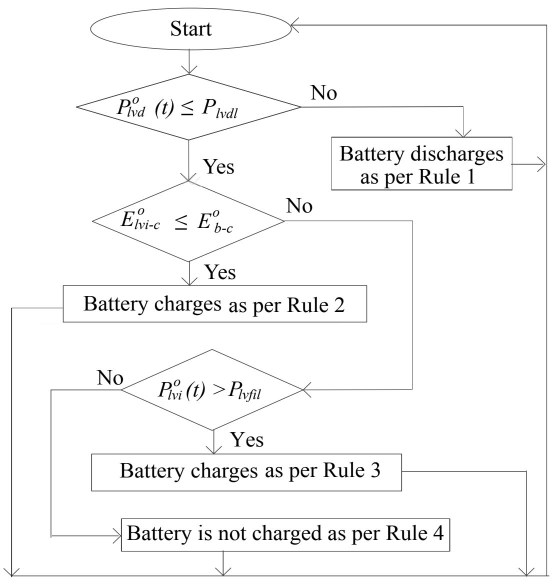

Fig. 4. Determination of the battery charge/discharge schedules using the proposed rule-based peak shaving control.

subjected to

1) Power balance constraint

$$P_{dgb}(t) + P_b(t) = P_{lv}(t). \tag{32}$$

2) Battery SoC Constraints

$$SoC_l \leq SoC(t) \leq SoC_u, SoC_f = SoC_i. \tag{33}$$

3) Battery charge/discharge power constraints

$$P_{b-c}(t) \leq P^l_{b-c}, P_{b-d}(t) \leq P^l_{b-d}. \tag{34}$$

4) Battery energy capacity constraint

$$E^*_{b-d} \leq E_{b-r}. \tag{35}$$

5) Constraint of available energy to charge the battery

$$E_{dg-c} + E^o_{lvi-c} \geq E_{b-c}. \tag{36}$$

The E^*_{b-d} is considered as a control variable, since the control inputs of the peak shaving control depend on E^*_{b-d}. Note that determination of fitness function requires the DG powers over a day, which are determined using (6) and (32). For obtaining the battery schedules the proposed rules are used. The considered fitness function is non linear. Therefore, GA is used to solve the optimization problem. The population size is tuned such that multiple simulation runs converge precisely to the same value and chosen as 20. This population size is less as there is only one control variable in this optimization problem. The solution of this optimization problem provides optimal dischargeable energy of the battery and thus optimal control inputs of the peak shaving control.

VIII. Results

The simulation results are obtained using MATLAB. Firstly, the rating of DG is determined by testing the proposed peak shaving control in worst case scenario as discussed follows.

TABLE I
Battery parameters [30], [42]

Parameter	Value	Parameter	Value
η_c	0.95	SoC_l/SoC_u	0.2/0.9
η_d	0.95	SoC_i	0.5
E_{b-r}	400 kWh	P^l_{b-c}	100 kW
V_{b-r}	120 V	P^l_{b-d}	100 kW

A. DG Rating

In general the rating of a device is chosen based on the worst operating conditions. In the proposed control, the DG is used to balance the deficit load demand (load demand that is not supplied by the RESs). The BESS is employed for peak shaving purpose while supplying the deficit load demand along with DG. Moreover, BESS involves energy capacity rating. In this scenario, the worst operating conditions occur when the daily deficit load demand is maximum, and individual load demands are such that their peak power values coincide over the day. In order to reflect this scenario, it is considered that RESs power is not available over the entire day. Further, load profiles are considered such that all the loads are operating at its peak during 9:00 and 12:00 hours over a day [41]. In this case the total load power is shown in Fig. 5(a). The total energy of load demand over the day is 2010 kWh. Note that the DG rating is determined without considering any contingencies. The results during this scenario are discussed as follows.

1) Slave Level Optimization: In this level the optimal LV ac bus power values over a day are determined. The determined V^o_{lv} is 1.05 p.u. for all the times as shown in Fig. 5(b). This is because there is no RESs power in this case. Moreover, there is no reactive power supplied by RES converters due to the absence of RESs power. In this situation there will be only voltage drop scenario. Therefore, the minimum load bus voltage profile which is occurring at L5 is shown in Fig. 5(c). The load bus voltages are above 0.95 p.u. which indicates that there are no voltage drop violations. The resulting optimal LV ac bus power values are shown in Fig. 5(d). It indicates that the peak optimal LV ac bus power is 189.0215 kW.

2) Rule-based Peak Shaving Control with Master Level Optimization: The optimal LV ac bus power values obtained from the slave level optimization are used as inputs to the rule-based peak shaving control. Using these LV ac bus power values, the optimal control inputs are obtained with the help of master level optimization. The best fitness values are obtained for multiple runs of GA as shown in Fig. 6. It shows that the minimum value for all the runs is equal to 137.825 kW which is the optimal peak DG power ($P^o_{dg-peak}$). The optimal dischargeable energy of the battery is found to be 194.8388 kWh. The corresponding control inputs i.e., P^o_{lvdl}, E^o_{b-c}, E^o_{lvi-c}, E^o_{dg-c} and C^o_{dg} are 137.825 kW, 194.8388 kWh, 0 kWh, 1380.6 kWh and 0.1411, respectively. The P^o_{lvfil} is not applicable in this case as there is no injected LV ac bus power available. The optimal LV ac bus powers are shown in Fig. 7(a). The charge/discharge schedules of the battery along with its SoC are shown in Fig. 7(b). This shows that the battery power and SoC are maintained within their limits. Moreover, SoC at the end of the day is maintained equal to the SoC

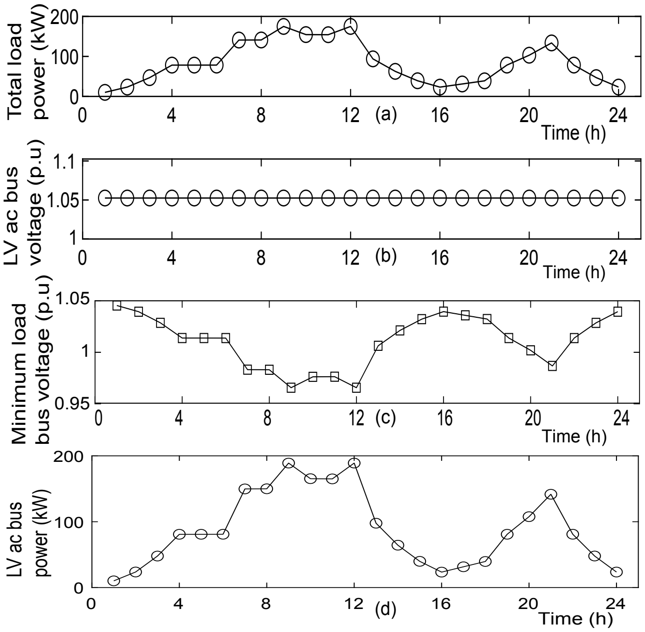

Fig. 5. Slave level optimization while determining rating of DG. (a) Total load power [41]. (b) LV ac bus voltage. (c) Minimum load bus voltage. (d) Optimal LV ac bus power.

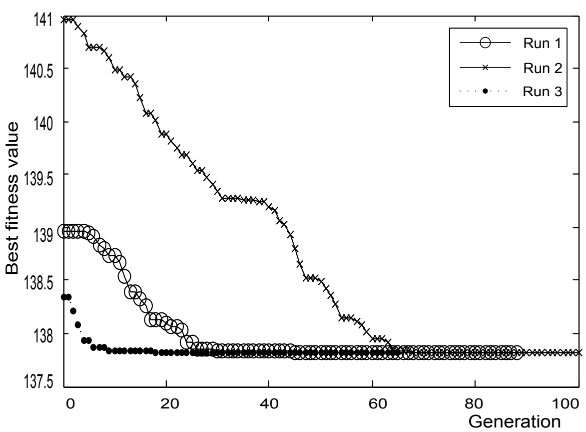

Fig. 6. Best fitness values of GA with master level optimization while determining the rating of DG.

of start of the day to ensure flexible day to day management of the battery. The resulting DG power is shown in Fig 7(c). This shows that DG power is limited to P^{o}_{lvdl} of 137.8249 kW which justifies the proposed peak shaving control. This peak DG bus power which is obtained in worst operating conditions is considered as the DG rating.

3) Impact of the Proposed Peak Shaving Control On DG Rating: The comparison of this DG rating with respect to base case (when there is no minimization of the LV ac bus power and no peak shaving control) and with respect to the case when there is only LV ac bus power minimization without peak shaving control [14]–[17] is given in Table II. It shows that the DG rating is 190.6915 kW for base case and 189.0215 kW with only LV ac bus power minimization without peak shaving control. This indicates that the DG power rating is reduced by 27.09% with the proposed peak shaving control as compared to the case when there is only LV ac bus power minimization.

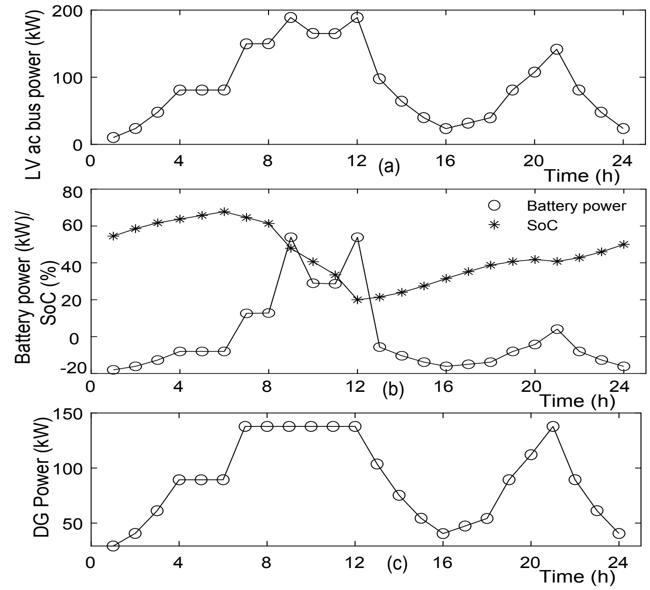

Fig. 7. Rule-based peak shaving control while determining rating of DG. (a) Optimal LV ac bus power. (b) Charge/discharge powers and SoC of the battery. (c) DG power.

TABLE II
DG RATING

Method	P_{dg-r} (kW)
Base case	190.6915
Minimization of LV ac bus power without the peak shaving [14]–[17]	189.0215
Minimization of LV ac bus power along with the proposed peak shaving	137.8249

As per the proposed peak shaving control, two different possible cases exist considering the RESs characteristics. The first case is when the available optimal LV ac bus injected energy to charge the battery is less than or equal to required energy to charge the battery over a day. The second case is when the available optimal LV ac bus injected energy to charge the battery is more than the required energy to charge the battery over a day. The results of the rule-based control for the first possible case are verified while determining the rating of DG. In order to verify the second case and show the impact of the proposed peak shaving control on fuel consumption of DG and self consumption rate of the system a case study is considered as given follows.

B. Case Study

The performance of the proposed method is tested in this case considering the day-ahead forecasts of load and RES powers as inputs. The day-ahead load powers are considered such that they are operating at half of their peak loads during 9:00 and 12:00 hours of the day. The total energy of load demand over the day is 1005 kWh. The day-ahead RES powers are considered such that they are operating at their installed capacities during their maximum power generation hours. The

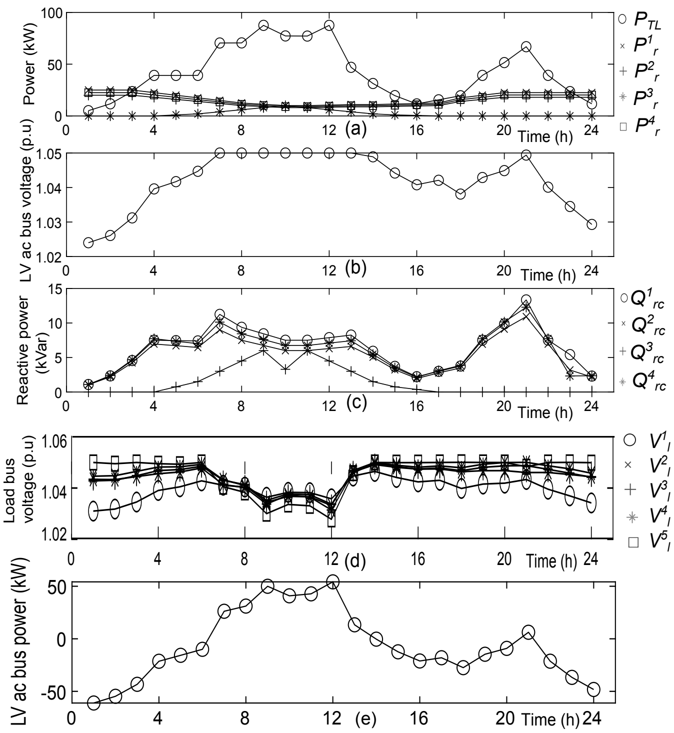

Fig. 8. Slave level optimization during case study analysis. (a) Total load and RES powers [41], [43]. (b) LV ac bus voltage. (c) Reactive power of RES converters. (d) Load bus voltages (e) Optimal LV ac bus power.

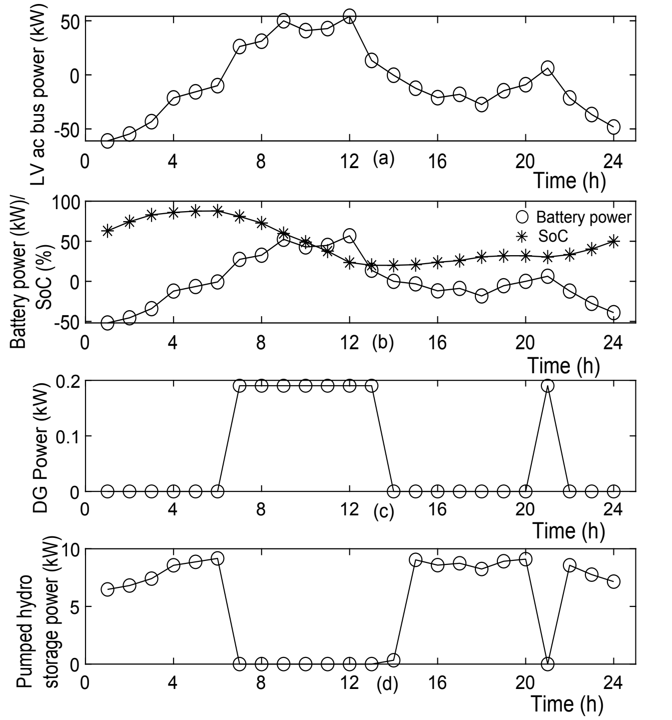

Fig. 9. Rule-based peak shaving control during case study analysis. (a) Optimal LV ac bus power. (b) Charge/discharge powers and SoC of the battery. (c) DG power. (d) PHS power.

total energy of RESs over the day is 1165.5 kWh . The total load power and RESs power profiles are shown in Fig. 8(a) [41], [43]. The obtained results are discussed as follows.

1) Slave Level Optimization: The determined V_{lv}^{o} and Q_{rc}^{oj} are shown in the Fig. 8(b) and Fig. 8(c) , respectively. These indicate that the voltage at the LV ac bus and reactive power supplied by RES converters are controlled as per the variation of load and RESs power. For this case there will be both voltage rise and voltage drop conditions due to the presence of RESs power. Therefore, all the load bus voltage profiles are shown in Fig. 8(d). This indicates that there are no voltage drop and voltage rise violations as load bus voltages are within 0.95 p.u. and 1.05 p.u. at all the hours of the day. The resulting optimal LV ac bus power values over a day are shown in Fig. 8(e). It indicates that the peak optimal LV ac bus power is 54.1876 kW.

2) Rule-based Peak Shaving Control with Master Level Optimization: The resulting day-ahead optimal LV ac bus power profile obtained from the slave level optimization is the input to rule-based peak shaving control as shown in Fig. 9(a). Using this optimal LV ac bus power profile, the determined optimal control inputs i.e., P_{lvdl}^{o}, E_{b-c}^{o}, E_{lvi-c}^{o} and P_{lvfil}^{o} are 0.1904 kW, 277.1157 kWh, 415.4510 kWh and 9.2067 kW, respectively. In this case E_{lvi-c}^{o} is more than E_{b-c}^{o}. Therefore, E_{dg-c}^{o} and C_{g-c}^{o} are not applicable. For these inputs the charge/discharge schedules of the battery along with its SoC are shown in Fig. 9(b). This shows that the battery power and SoC are maintained within their limits. Moreover, SoC at the end of the day is maintained equal to the SoC of start of the day to ensure flexible day to day management of the battery. The resulting DG power is shown in Fig 9(c). This shows that the DG power is limited to P_{lvdl}^{o} of 0.1904 kW. The resulting PHS power is shown in Fig. 9(d). This shows that the PHS power is limited to P_{lvfil}^{o} of 9.2067 kW. This justifies the proposed peak shaving control method.

This paper aims to show the impact of the proposed rule-based peak shaving control on DG supplied distribution system without considering the uncertainties in the day-ahead predictions of load and RES powers. In case if the actual load and RES power values are different from the day-ahead predictions due to uncertainties, the peak DG power may not be limited to the optimal demand limit and flexible day-to-day management of the battery may not be maintained. The real-time implementation method considering this impact of uncertainties is the future scope of this work.

3) Impact of the Proposed Peak Shaving Control on Total Fuel Consumption of DG: The total fuel consumption of DG over a day is calculated using (37),

$$TFC_{dg} = \sum_{t=1}^{T} [(a \times P_{dg}(t)) + (b \times P_{dg-r})]. \qquad (37)$$

The TFC_{dg} without minimization of LV ac bus power and without the peak shaving control is calculated as 451.4965 L. The TFC_{dg} with only LV ac bus power minimization without the peak shaving control is 446.8858 L. However, with LV ac bus power minimization and the proposed peak shaving control TFC_{dg} is calculated as 278.7257 L. This indicates that the fuel consumption is reduced by 37.63% with the proposed peak shaving control as compared to the case when there is only LV ac bus power minimization.

TABLE III
FUEL CONSUMPTION AND SELF CONSUMPTION RATES FOR CASE STUDY

Method	TFC_{dg} (L)	SCR
Base case	451.4965	0.6453
Minimization of LV ac bus powers without the peak shaving [14]–[17]	446.8858	0.6436
Minimization of LV ac bus powers along with the proposed peak shaving	278.7257	0.8938

4) Impact of the proposed Peak Shaving Control On Self Consumption Rate: Self consumption rate is defined as the ratio of self consumed RESs energy and total generated RESs energy [44] i.e.,

$$SCR = \frac{E_r - E_{phs}}{E_r}. \quad (38)$$

The SCR without minimization of LV ac bus power and without the peak shaving control is calculated as 0.6453. The SCR with only LV ac bus power minimization without the peak shaving control is 0.6436. However, with LV ac bus power minimization and the proposed peak shaving control SCR is calculated as 0.8938. This indicates that the fuel consumption is increased by 38.88% with the proposed peak shaving control as compared to the case when there is only LV ac bus power minimization.

The quantitative comparison considering TFC_{dg} and SCR is shown in Table III.

IX. CONCLUSIONS

In this paper, peak shaving is achieved using optimal control of battery energy storage in diesel generator supplied isolated microgrid. The low voltage ac bus power requirement is minimized through a slave level optimization and the rule-based control is optimized through a master level optimization. It is observed that the diesel generator rating is reduced by 27.09% with the proposed peak shaving control as compared to the case when there is only low voltage ac bus power minimization. Further, it is observed that the fuel consumption of diesel generator is reduced by 37.63% and self consumption rate is increased by 38.88% with the proposed peak shaving control method as compared to the case when there is only low voltage ac bus power minimization.

REFERENCES

[1] S. Mashayekh, M. Stadler, G. Cardoso, M. Heleno, S. C. Madathil, H. Nagarajan, R. Bent, M. Mueller-Stoffels, X. Lu, and J. Wang, "Security-constrained design of isolated multi-energy microgrids," *IEEE Trans. Power Syst.*, vol. 33, no. 3, pp. 2452–2462, 2018.

[2] H. V. M., A. K. Deka, and C. Kumar, "Capacity enhancement of a radial distribution grid using smart transformer," *IEEE Access*, vol. 8, pp. 72 411–72 423, 2020.

[3] R. D. Trevizan, A. Stanley, J. H. Alexander, G. Robert, and G. Imre, "Integration of energy storage with diesel generation in remote communities," *MRS Energy Sustainability*, vol. 8, pp. 57–74, 2021.

[4] Y. Yoldas, S. Goren, and A. Onen, "Optimal control of microgrids with multi-stage mixed-integer nonlinear programming guided ¡tex¿q¡/tex¿-learning algorithm," *J. Mod. Power Syst. Clean Energy.*, vol. 8, no. 6, pp. 1151–1159, 2020.

[5] B. Khan and P. Singh, "Selecting a meta-heuristic technique for smart micro-grid optimization problem: A comprehensive analysis," *IEEE Access*, vol. 5, pp. 13 951–13 977, 2017.

[6] Y. A. Katsigiannis, P. S. Georgilakis, and E. S. Karapidakis, "Hybrid simulated annealing–tabu search method for optimal sizing of autonomous power systems with renewables," *IEEE Trans. Sustain. Energy*, vol. 3, no. 3, pp. 330–338, 2012.

[7] A. Q. Mohammed, K. A. Al-Anbarri, and R. M. Hannun, "Optimal combination and sizing of a stand–alone hybrid energy system using a nomadic people optimizer," *IEEE Access*, vol. 8, pp. 200 518–200 540, 2020.

[8] H. V. M., D. Das, C. Kumar, H. B. Gooi, M. Saad, and X. Guo, "Increasing voltage support using smart power converter based energy storage system and load control," *IEEE Trans. Ind. Electron.*, vol. 68, no. 12, pp. 12 364–12 374, 2021.

[9] B. Singh, R. Niwas, and S. K. Dube, "Load leveling and voltage control of permanent magnet synchronous generator-based dg set for standalone supply system," *IEEE Trans. Ind. Informat.*, vol. 10, no. 4, pp. 2034–2043, 2014.

[10] K. Kant, C. Jain, and B. Singh, "A hybrid diesel-windpv-based energy generation system with brushless generators," *IEEE Trans. Ind. Informat.*, vol. 13, no. 4, pp. 1714–1722, 2017.

[11] S. Lakshmi and S. Ganguly, "An on-line operational optimization approach for open unified power quality conditioner for energy loss minimization of distribution networks," *IEEE Trans. Power Sys.*, vol. 34, no. 6, pp. 4784–4795, 2019.

[12] N. Wang, J. Li, W. Hu, B. Zhang, Q. Huang, and Z. Chen, "Optimal reactive power dispatch of a full-scale converter based wind farm considering loss minimization," *Renew. Energy*, vol. 139, pp. 292–301, 2019.

[13] V. Sarfi and H. Livani, "Optimal volt/var control in distribution systems with prosumer ders," *Electr. Power Syst. Res.*, vol. 188, p. 106520, 2020.

[14] G. De Carne, G. Buticchi, M. Liserre, and C. Vournas, "Load control using sensitivity identification by means of smart transformer," *IEEE Trans. Smart Grid*, vol. 9, no. 4, pp. 2606–2615, 2018.

[15] J. Chen, M. Liu, G. De Carne, R. Zhu, M. Liserre, F. Milano, and T. O'Donnell, "Impact of smart transformer voltage and frequency support in a high renewable penetration system," *Electr. Power Syst. Res.*, vol. 190, p. 106836, 2021.

[16] R. Anilkumar, G. Devriese, and A. K. Srivastava, "Voltage and reactive power control to maximize the energy savings in power distribution system with wind energy," *IEEE Trans. Ind. Appl.*, vol. 54, no. 1, pp. 656–664, 2018.

[17] R. R. Jha, A. Dubey, C.-C. Liu, and K. P. Schneider, "Bi-level volt-var optimization to coordinate smart inverters with voltage control devices," *IEEE Trans. Power Syst.*, vol. 34, no. 3, pp. 1801–1813, 2019.

[18] L. Bhamidi and S. Sivasubramani, "Optimal planning and operational strategy of a residential microgrid with demand side management," *IEEE Syst. J.*, vol. 14, no. 2, pp. 2624–2632, 2020.

[19] N. Chakraborty, A. Mondal, and S. Mondal, "Efficient scheduling of nonpreemptive appliances for peak load optimization in smart grid," *IEEE Trans. Ind. Informat.*, vol. 14, no. 8, pp. 3447–3458, 2018.

[20] S. Zhao, X. Lin, and M. Chen, "Robust online algorithms for peak-minimizing ev charging under multistage uncertainty," *IEEE Trans. Automat. Contr.*, vol. 62, no. 11, pp. 5739–5754, 2017.

[21] W. Wu, Y. Lin, R. Liu, Y. Li, Y. Zhang, and C. Ma, "Online ev charge scheduling based on time-of-use pricing and peak load minimization: Properties and efficient algorithms," *IEEE Trans. Intell. Transp. Syst.*, vol. 23, no. 1, pp. 572–586, 2022.

[22] Y. Mo, Q. Lin, M. Chen, and S. J. Qin, "Optimal peak-minimizing online algorithms for large-load users with energy storage," in *IEEE INFOCOM 2021 -IEEE Conf. Comput. Commun. Workshops (INFOCOM WKSHPS)*, 2021, pp. 1–2.

[23] K. Mahmud, M. J. Hossain, and G. E. Town, "Peak-load reduction by coordinated response of photovoltaics, battery storage, and electric vehicles," *IEEE Access*, vol. 6, pp. 29 353–29 365, 2018.

[24] D. M. Greenwood, N. S. Wade, P. C. Taylor, P. Papadopoulos, and N. Heyward, "A probabilistic method combining electrical energy storage and real-time thermal ratings to defer network reinforcement," *IEEE Trans. Sustain. Energy*, vol. 8, no. 1, pp. 374–384, 2017.

[25] D. T. Vedullapalli, R. Hadidi, and B. Schroeder, "Combined hvac and battery scheduling for demand response in a building," *IEEE Trans. Ind. Appl.*, vol. 55, no. 6, pp. 7008–7014, 2019.

[26] N. Ahmed, M. Levorato, and G. P. Li, "Residential consumer-centric demand side management," *IEEE Trans. Smart Grid*, vol. 9, no. 5, pp. 4513–4524, 2018.

[27] Y. Guo, Q. Zhang, and Z. Wang, "Cooperative peak shaving and voltage regulation in unbalanced distribution feeders," *IEEE Trans. Power Syst.*, vol. 36, no. 6, pp. 5235–5244, 2021.

[28] J. von Appen, T. Stetz, M. Braun, and A. Schmiegel, "Local voltage control strategies for pv storage systems in distribution grids," *IEEE Trans. Smart Grid*, vol. 5, no. 2, pp. 1002–1009, 2014.

[29] G. Angenendt, S. Zurmühlen, R. Mir-Montazeri, D. Magnor, and D. U. Sauer, "Enhancing battery lifetime in pv battery home storage system using forecast based operating strategies," *Energy Procedia*, vol. 99, pp. 80–88, 2016, 10th International Renewable Energy Storage Conference, IRES 2016, 15-17 March 2016, Düsseldorf, Germany.

[30] R. Manojkumar, C. Kumar, S. Ganguly, and J. P. S. Catalão, "Optimal peak shaving control using dynamic demand and feed-in limits for grid-connected pv sources with batteries," *IEEE Syst. J.*, vol. 15, no. 4, pp. 5560–5570, 2021.

[31] Cigre Task Force C6.04.02, "Benchmark systems for network integration of renewable and distributed energy resources," Tech. Rep., Apr. 2014.

[32] B. Zhao, X. Zhang, J. Chen, C. Wang, and L. Guo, "Operation optimization of standalone microgrids considering lifetime characteristics of battery energy storage system," *IEEE Trans. Sustain. Energy*, vol. 4, no. 4, pp. 934–943, 2013.

[33] H. Mehrjerdi, R. Hemmati, M. Shafie-khah, and J. P. S. Catalao, "Zero energy building by multi-carrier energy systems including hydro, wind, solar and hydrogen," *IEEE Trans. Ind. Informat.*, pp. 1–1, 2020.

[34] K. Y. Bae, H. S. Jang, and D. K. Sung, "Hourly Solar Irradiance Prediction Based on Support Vector Machine and Its Error Analysis," *IEEE Trans. Power Syst.*, vol. 32, no. 2, pp. 935–945, 2017.

[35] K. Amasyali and N. M. El-Gohary, "A review of data-driven building energy consumption prediction studies," *Renew. Sust. Energ. Rev.*, vol. 81, pp. 1192–1205, 2018.

[36] M. Xia, H. Shao, X. Ma, and C. W. de Silva, "A Stacked GRU-RNN-Based Approach for Predicting Renewable Energy and Electricity Load for Smart Grid Operation," *IEEE Trans. Ind. Informat.*, vol. 17, no. 10, pp. 7050–7059, 2021.

[37] R. Manojkumar, C. Kumar, S. Ganguly, H. B. Gooi, and S. Mekhilef, "Voltage control using smart transformer via dynamic optimal setpoints and limit tolerance in a residential distribution network with pv sources," *IET Gener. Transm. Distrib.*, vol. 14, no. 22, pp. 5143–5151, 2020.

[38] T. Chau, P. Burovskiy, M. Flynn, and W. Luk, "Chapter two - advances in dataflow systems," ser. Adv. Comput., A. R. Hurson and V. Milutinović, Eds. Elsevier, 2017, vol. 106, pp. 21–62.

[39] V. Kumar, J. K. Chhabra, and D. Kumar, "Parameter adaptive harmony search algorithm for unimodal and multimodal optimization problems," *J. Comput. Sci.*, vol. 5, no. 2, pp. 144–155, 2014.

[40] S. Areibi, M. A. Moussa, and G. Koonar, "A Genetic Algorithm Hardware Accelerator for VLSI Circuit Partitioning," *Int. J. Comput. Their Appl.*, vol. 12, pp. 163–180, 2005.

[41] K. Gaur, H. Kumar, R. P. K. Agarwal, K. V. S. Baba, and S. K. Soonee, "Analysing the electricity demand pattern," in *2016 Nat. Power Syst. Conf. (NPSC)*, 2016, pp. 1–6.

[42] D. Bryans, V. Amstutz, H. H. Girault, and L. E. A. Berlouis, "Characterisation of a 200 kW/400 kWh Vanadium Redox Flow Battery," *Batteries*, vol. 4, no. 4, 2018.

[43] V. K. Agrawal, A. Khemka, K. Manoharan, D. Jain, and S. Mukhopadhyay, "Wind-solar hybrid system — an innovative and smart approach to augment renewable generation and moderate variability to the grid," in *2016 IEEE 7th Power India Int. Conf. (PIICON)*, 2016, pp. 1–5.

[44] K. P. Satsangi, D. B. Das, G. S. Babu, and A. Saxena, "Real time performance of solar photovoltaic microgrid in india focusing on self-consumption in institutional buildings," *Energy Sustain Dev*, vol. 52, pp. 40–51, 2019.

Rampelli Manojkumar (Student Member, IEEE) received the B.E. degree in electrical and electronics engineering from Vasavi College of Engineering, Hyderabad, India, in 2013, and the M.Tech. degree in power and energy systems from the National Institute of Technology Karnataka, Surathkal, India, in 2015. He is currently working toward the doctoral degree with the Department of Electronics and Electrical Engineering, Indian Institute of Technology Guwahati, India. His research interests are optimal energy management, hybrid distribution systems.

Chandan Kumar (Senior Member, IEEE) received the Ph.D. degree from the Indian Institute of Technology Madras, India, in 2014 in electrical engineering. During 2016 to 2017, he was an Alexander von Humboldt Research Fellow with the Chair of Power Electronics, University of Kiel, Kiel, Germany. He is currently an Associate Professor in the Department of Electronics and Electrical Engineering in Indian Institute of Technology Guwahati, India. His research interests are power electronics application in power system, power quality, and renewable energy.

Sanjib Ganguly (Senior Member, IEEE) received M.E. degree in electrical engineering from Jadavpur University, India in 2006. He received the Ph.D degree from Indian Institute of Technology Kharagpur, India in 2011. He is currently an Associate Professor in the Department of the Electronics and Electrical Engineering in Indian Institute of Technology Guwahati, India. His research interests are power system operation and planning, custom power devices, hybrid energy system, and evolutionary algorithms.

Hoay Beng Gooi (Life Senior Member, IEEE) received the Ph.D. degree from Ohio State University, Columbus, OH in 1983 in electrical engineering. He is presently working as an Associate Professor with the School of Electrical and Electronic Engineering, NTU. He has served as Co-Director of SP Group-NTU Joint Lab since 2019. His current research interests include microgrid energy management systems dealing with energy storage, condition monitoring, electricity market, and spinning reserve.

Saad Mekhilef (Fellow, IEEE) is currently a Distinguished Professor with the School of Science, Computing and Engineering Technologies, Swinburne University of Technology, Australia, and an Honorary Professor with the Department of Electrical Engineering, University of Malaya. He authored and coauthored more than 500 publications with more than 33,000 citations. His research interests include power conversion techniques, control of power converters, maximum power point tracking (MPPT), renewable energy, and energy efficiency.

João P. S. Catalão (Fellow, IEEE) received the M.Sc. degree from the Instituto Superior Técnico, Lisbon, Portugal, in 2003, and the Ph.D. and Habilitation degrees for Full Professor from the University of Beira Interior, Covilhã, Portugal, in 2007 and 2013, respectively. He is currently a Professor with the Faculty of Engineering, University of Porto, Porto, Portugal, and a Research Coordinator with INESC TEC. His research interests include power system operations and planning, distributed renewable generation, demand response, and smart grids.